Environ. Sci. Technol. **2004**, *38,* 4149−4156

Solar Photodecomposition of Decabromodiphenyl Ether: Products and Quantum Yield

JUAN BEZARES-CRUZ,
CHAD T. JAFVERT,* AND INEZ HUA
School of Civil Engineering, Purdue University, West Lafayette, Indiana 47907-1284

Decabromodiphenyl ether (BDE209) is a widely used flame retardant, yet information regarding its environmental transformation rates and pathways are largely unknown. Because photochemical transformation is often suggested as a potentially important fate process for BDE209, the reaction rate and products of the solar degradation under favorable solvent conditions were determined in this study. Decabromodiphenyl ether (BDE209), dissolved in hexane, reacts in minutes via direct solar irradiation, at midlatitude (40°29′ N, 86°59.5′ W) in afternoon July and October sunlight. Observed first-order reaction rate constants, k_{obs}, at the different exposure times were $k_{obs} = 1.86 \times 10^{-3}$ s^{-1} (July) and $k_{obs} = 1.11 \times 10^{-3}$ s^{-1} (October). The photodecomposition quantum yield was calculated from these data and from the solar irradiance data measured at 300, 305.5, 311.4, 317.6, 325.4, 332.4, and 368 nm reported at a USGS UVB monitoring station located nearby. The range of wavelengths where both the molar absorptivity of BDE209 and the solar irradiance flux are significant occurs between 300 and 350 nm. For this range, the wavelength average quantum yield for BDE209 photoreaction, ϕ_{ave}, was calculated to be 0.47. The difference between k_{obs} values at the two exposure times is explained fully by the difference between the solar irradiation fluxes. Upon solar irradiation, BDE209 reductively dehalogenated to other polybrominated diphenyl ethers (PBDEs). During 34 h of irradiation, PBDEs ranging from nona- to tribromodiphenyl ethers were observed. In total, 43 PBDEs were detected, and the GC retention times and mass spectral fragment patterns of 21 products matched those of available congener standards, including congeners 2,2′,4,4′,5-pentabromodiphenyl ether and 2,2′,4,4′-tetrabromodiphenyl ether.

Introduction

Polybrominated diphenyl ethers (PBDEs), a class of brominated flame retardants, have recently been extensively investigated as environmental contaminants. PBDEs have been detected in various environmental media, including soil (*1*), sediment (*2*−*6*), air (*7*−*9*), and biota (*10*−*18*). In particular, the concentrations and the distribution profiles of the various PBDE congeners have been widely reported in the United States, Europe, and Japan (*19*), as well as in more remote locations, including the Canadian Arctic (*20*).

The partitioning of PBDEs to various phases and surfaces has also been measured or modeled. For example, recent studies have reported or predicted partitioning to soot particles (*21*), aerosols (*8*, *22*, *23*), leaf-litter (*7*), and organic films collected from windows (*24*). Complementing the partitioning and transport studies are reports of selected physical−chemical properties of various PBDEs, including octanol−air partition coefficients (*22*, *25*, *26*) and vapor pressures (*23*, *27*). Most of these studies indicate that PBDEs, particularly those congeners with a greater number of bromine atoms, will preferentially accumulate into phases of an organic (hydrophobic) nature.

There is some uncertainty, however, as to how congener profiles observed in the environment can be reconciled with those of commercial formulations. There are three formulations of PBDEs that are incorporated in consumer products: penta, octa, and deca formulations. The congener profiles in each formulation are discussed in detail elsewhere (*28*−*30*); however, the deca formulation is generally >95% decabromodiphenyl ether (BDE209). The annual global production of the PBDEs is about 67 000 t, with the deca formulation accounting for over 80% of the total (*31*). In most cases, the congener profiles detected in environmental samples include very little if any BDE209 and generally match the congener distribution of the penta formulation more closely. One possible explanation is that the higher molecular weight congeners, including BDE209, undergo reductive dehalogenation in the environment, producing many of the lower molecular weight congeners.

However, few published studies are available regarding biotic and abiotic transformation of PBDEs. This is especially true for BDE209. A recent study indicates biotic transformation of BDE209 in carp forms lower molecular weight PBDE congeners (*32*) and potentially in salmon forming hydroxylated PBDEs (*33*). Photolysis is a potential abiotic transformation mechanism in the environment and has been reported to occur under a variety of conditions (*34*−*36*). These reports include data utilizing both artificial and natural sunlight and in some cases demonstrate the debromination of BDE209 to other PBDEs; however, information regarding the identity and structure of specific congeners that form is very limited. The identities of the congeners produced during photochemical decomposition are important to gain insight into how congener profiles in environmental samples may relate back to potential release inventories of commercial formulations.

In this study, we present a quantitative study on the photochemical transformation of BDE209 dissolved in hexane. Experiments were conducted in solar light, the quantum yield of BDE209 photodecomposition under these conditions is calculated, and product distributions are described. The rationale for conducting these experiments in hexane rather than pure or natural waters is three-fold: first, with pure water as the solvent, the solubility of BDE209 and its partitioning to container walls from a pure aqueous solution precludes straightforward analysis of products and kinetic rates. Second, transparency to UVB light, solvency toward BDE209, and the ability to act as a hydrogen donor are favorable properties of hexane that suggest facile reaction in this solvent. Third, BDE209 partitioning to humic materials in natural systems is significant, and hexane is a reasonable surrogate (e.g., hydrogen donor) for these materials.

Materials and Methods

Materials. Decabromodiphenyl ether (BDE209; 98% purity) was obtained from Great Lakes Chemical Company. A mixture of 39 PBDE congeners (EO-5113), ranging in bromine substitution from one (mono-) to seven (hepta-), was

* Corresponding author phone: (765)494-2196; fax: (765)496-1107; e-mail: jafvert@ecn.purdue.edu.

10.1021/es049608o CCC: $27.50 © 2004 American Chemical Society
Published on Web 06/29/2004

purchased from Cambridge Isotope Laboratories, Inc. Seven individual congeners (BDE-77, -156, -184, -191, -196, -206, and -207) and an additional standard of BDE209, dissolved in hexane, were purchased from Wellington Laboratories. Analytical grade hexanes (87.8% *n*-hexane) and toluene were purchased from Mallinckrodt Chemicals. Octachloronaphthalene (OCN) and hexachlorobenzene were used as internal standards and purchased from AccuStandard Inc. and Sigma-Aldrich, respectively.

BDE209 Molar Absorptivity. Three solutions of BDE209 (6.92×10^{-6} to 6.14×10^{-6} μM) were prepared by dissolving known weights of crystal samples in hexane, sonicating for 10 s, and placing them in the dark for 24 h prior to measurement. Molar absorptivities were measured with matched 10 cm path length quartz cuvettes in a Perkin-Elmer Lambda 20 spectrophotometer at 1 nm intervals. The reported absorptivities are the average of the three measurements.

Solar Irradiation in Hexane. Solutions of BDE209 dissolved in hexane were exposed to solar light on the roof of the Civil Engineering Building at Purdue University (West Lafayette, IN; 40°26′ N, 86°55′ W). For each sample that was irradiated, an identical dark control sample was prepared and covered with aluminum foil and black felt and sampled at the same time as its corresponding irradiated sample. Duplicate samples were prepared.

To measure the reaction rate, kinetic experiments were conducted on July 2, 2003 at 2:50 to 3:10 p.m. and on October 23, 2003 at 1:44 to 2:39 p.m, with the initial BDE209 concentration within the range of 2−5 μM. For each experiment, small aliquots of stock solution were transferred to a series of 1 cm diameter, 9 mL screw-top Pyrex test tubes and exposed to sunlight. Tubes were removed from the light over time and analyzed for remaining BDE209.

To determine reaction products by GC−MS, large quantities of the same stock solutions were irradiated with sunlight for longer periods of time than for the kinetics experiments. Typically, samples were exposed to sunlight on clear days from 10 a.m. to 5 p.m. from July 2 to 23, 2003 or from October 23 to November 3, 2003. Samples were irradiated in 660 mL quartz vessels; the initial volume of each sample was 250 mL. The maximum time of exposure was 34 h over 7 days. Over time, 1 mL subsamples were removed from photolyzed and dark control vessels and placed in 2 mL amber vials for direct gas chromatographic analysis.

Solar Irradiation of Selected Lower PBDE Congeners in Hexane. The photoreactivities of several other congeners were examined by irradiating individual congeners dissolved in hexane from 2 p.m. on January 8 to noon the next day. Solutions of BDE-156, -184, -191, -196, -206, and -207 (0.5 mg/L each) were prepared, placed in 9 mL Pyrex tubes as described previously (individually), and irradiated and sampled as described previously.

Chemical Analysis. Samples were analyzed with a Hewlett-Packard 5890 II gas chromatograph (GC) equipped with an electron capture detector (ECD), a programmable pressure on-column injector, and a ZB5 capillary column (Phenomenex; length = 15 m, i.d. = 0.25 mm, film thickness = 0.1 μm). The carrier gas was He, and the makeup gas was N_2. The oven temperature was programmed from 150 °C (held for 2 min) to 280 °C at a rate of 10 °C/min; the final temperature was maintained for 30 min. The molecular masses and bromine content of compounds produced during photolysis were determined with a Thermo Finnegan Polaris Q GC−MS, equipped with an ion-trap quadrupole mass spectrometer (MS). Electron impact ionization (EI) was utilized in the MS, and the column was a DB5-MS (Agilent/J&W; length = 25 m, i.d. = 0.25 mm, film thickness = 0.25 μm). The oven temperature program was identical to that of the GC-ECD system. Octachloronaphthalene (OCN) was used as an internal standard.

Quantum Yield Analysis. The USDA UV-B Monitoring and Research Program, headquartered at the Natural Resource Ecology Laboratory, Colorado State University, maintains a UVB monitoring station at the Purdue Agronomy Research Center Site (40°29′ N, 86°59.5′ W). The site is less than one mile from the Civil Engineering Building where samples were irradiated. At the monitoring station, diffuse, direct, and total irradiance are measured with a pyrometer at 300, 305.5, 311.4, 317.6, 325.4, 332.4, and 368 nm at 3 min intervals. The solar energy flux data from this site, corresponding to each kinetic experiment's irradiation period, were obtained to calculate the corresponding photon flux at each wavelength.

The energy of an einstein (of photons), E (joules/einstein), at a given wavelength, λ (nm), is given by

$$E = j\,\frac{hc}{\lambda} \tag{1}$$

where h is Planck's constant (6.626×10^{-34} J s); c is the speed of light (3×10^{8} m/s); and j is the number of photons per einstein (einstein = 6.022×10^{23} photons). Dividing the solar intensity (J m^{-2} nm^{-1} s^{-1})) by the energy of an einstein of light at each respective wavelength (J/einstein) results in the photon flux per area at the Earth's surface at each wavelength, denoted by $I_{o,\lambda}$ (einstein cm^{-2} nm^{-1} s^{-1})). Values of $I_{o,\lambda}$ measured with pyrometers differ slightly from solar flux values calculated via test tube actinometry studies due to light attenuation within test tubes by absorbing solutes and solvents, light reflectance and refraction, and absorption by the tube walls. For cylindrical tubes with no particles or absorbing species other than trace quantities of the test compound, Leifer (*37*) reports these effects to be generally less than a factor of 2.

BDE209's (base-10) molar absorptivity, ϵ_λ, is negligible above 353 nm. Similarly, solar light intensities at wavelengths less that 300 nm may be considered negligible. Over the range of 300−353 nm, and with initially only BDE209 in solution, the following rate law applies

$$-\frac{\mathrm{d}C}{\mathrm{d}t} = \int_{\lambda=300\mathrm{nm}}^{\lambda=353\mathrm{nm}} \phi_\lambda I_{o,\lambda}\left(\frac{A}{V}\right)(1 - 10^{-\epsilon_\lambda C l_{eff}})\,\mathrm{d}\lambda \tag{2}$$

where C is the molar concentration of BDE209, t is time, ϕ_λ is the quantum yield at wavelength λ, A/V is the exposed area to solution volume ratio, and l_{eff} is the effective path length. Eq 2 assumes $I_{o,\lambda}$ is constant over time, which is reasonable in sunlight for short exposure. Under conditions where $\epsilon_\lambda C l_{eff} < 0.05$, it can be shown through series expansion that

$$(1 - 10^{-\epsilon_\lambda C l_{eff}}) \cong \epsilon_\lambda C l_{eff} \log(10) \tag{3}$$

Upon substitution, the discrete approximation to eq 2 becomes

$$-\frac{\mathrm{d}C}{\mathrm{d}t} = \left(\frac{A l_{eff}}{V}\right)\left(2.303 \sum_{\lambda=300\mathrm{nm}}^{\lambda=353\mathrm{nm}} (\phi_\lambda I_{o,\lambda}\epsilon_\lambda)\right)C \tag{4}$$

For cylindrical tubes and with minimal light absorption by the solution, the effective path length is approximated by the geometric average path length through the tube, across its diameter. The cross-sectional area (diameter times height), multiplied by the geometric average path length through the tube, equals the solution volume ($A l_{eff}/V = 1$).

Over the range of applicable wavelengths from $\lambda = 300$−353 nm, it is reasonable to assume that the quantum yield is nearly independent of wavelength. Assuming the value of ϕ_λ is nearly constant ($=\phi_{ave}$) leads to

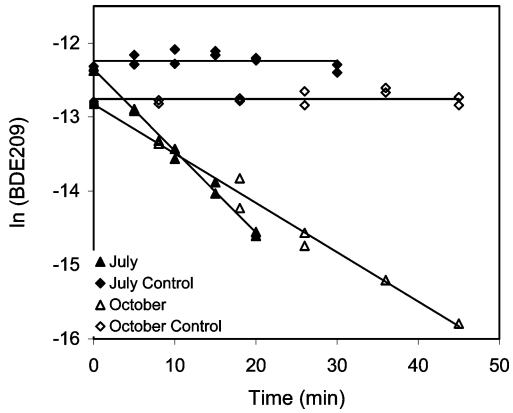

FIGURE 1. Photodecomposition of BDE209 in hexane by solar irradiation on July 2, 2003 and October 23, 2003.

$$-\frac{dC}{dt} = \phi_{ave} k_I C \quad (5)$$

where k_I (1/s) defines the first-order light absorption rate constant of the solute, BDE209.

$$k_I = 2.303 \sum_{\lambda=300nm}^{\lambda=353nm} (I_{o,\lambda}\, \epsilon_\lambda) \quad (6)$$

At each wavelength ($\Delta\lambda$ = 1 nm), the first-order light absorption rate constant, $k_{I,\lambda}$ (einstein/(mol nm s)), is

$$k_{I,\lambda} = 2.303 I_{o,\lambda} \epsilon_\lambda \quad (7)$$

Inspection of eq 5 shows that regression of ln(C) versus t results in a straight-line function with slope equal to $-k_I\phi_{ave}$, where k_I is determined independently from the measured molar absorptivities and solar flux data.

Results and Discussion

Reaction Kinetics. Figure 1 shows BDE209 dissolved in hexane decays within minutes upon irradiation with solar light. After 45 min of exposure to midafternoon sunlight on October 23, 2003, the BDE209 concentration was reduced to approximately 5% percent of the original concentration. The reaction was moderately faster on July 2 with less that 1% remaining after 30 min of exposure from 3:00 to 3:30 p.m. Also shown in Figure 1 are concentrations of BDE209 recovered from dark control samples collected over the same time periods. The concentration of BDE209 did not change in tubes not exposed to sunlight, indicating that photochemical reaction is occurring.

The data in Figure 1 show that on both days, the reaction followed first-order kinetics as predicted by eq 5, where the pseudo-first-order rate constant is proportional to the product of k_I and ϕ_{ave} integrated over all applicable wavelengths (eq 6). The molar absorptivities for BDE209, ϵ_λ, and the average solar intensities over the reaction periods on both days are plotted against λ in Figure 2a. At 300, 310, and 320 nm, the molar absorptivities in hexane were 2418, 2181, and 1142 M^{-1} cm^{-1}, respectively. At the experimental concentrations (<5 μM), the value of $\epsilon_\lambda C l_{eff}$ remains less than 0.01, satisfying the constraint on eq 3. The values of $I_{o,\lambda}$ at all wavelengths from 300 to 353 nm ($\Delta\lambda$ = 1 nm) were estimated by linear extrapolation between the measured values as indicated in Figure 2a. Values of $k_{I,\lambda}$, calculated from these values with eq 7 are shown in Figure 2b. Assuming that the quantum yield is nearly constant over these wavelengths, this figure indicated that light centered at λ = 320 nm is most responsible for BDE209 photodecomposition. For the July 2 and October 23 data, the integrated area under

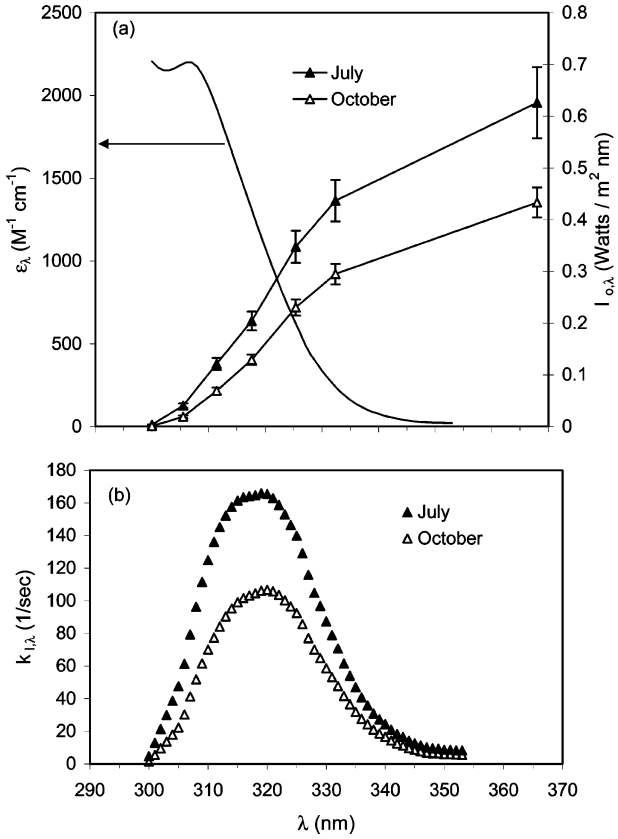

FIGURE 2. (a) BDE209 molar absorptivities and the average solar flux at West Lafayette, from 1:44 to 2:39 pm on October 23, 2003. (b) Absorbed solar light during the photolysis period.

the curve (=k_I) equals 4.13 × 10^{-3} and 2.58 × 10^{-3} einstein mol^{-1} s^{-1}, respectively. The corresponding pseudo-first-order reaction rate constants, k_{obs}, determined for the data in Figure 1 are 1.86 × 10^{-3} and 1.11 × 10^{-3} s^{-1}, respectively. The calculated average reaction quantum yields for the two sampling periods ($\phi_{ave} = k_{obs}/k_I$) are 0.48 and 0.46, respectively. Hence, the difference in reaction rates can be accounted for by the difference in solar intensities at the two exposure times. The rather large value of ϕ_{ave} is not unexpected, as the photons within this wavelength range are of sufficient energy to break most aryl carbon−bromine bonds. Also important is the transparency of hexane within this wavelength region and its ability to participate in the overall reaction as a hydrogen donor, which becomes apparent upon examining reaction intermediates and products.

Reaction Products. During solar irradiation in hexane, BDE209 undergoes reductive dehalogenation to form other congeners. To identify as many of these products as possible, GC retention times and mass spectra of the products were compared to those of standards. Table 1 contains the retention times and some other information for those PBDE standards available for this study. Over 40 PBDEs were observed during solar irradiation of BDE209 (Tables 2 and 3), and over 21 of these had identical retention times and mass spectra as specific PBDE standards. Those congeners found in irradiated samples whose mass spectra and GC retention times matched one of the known standards are reported in Tables 2 and 3 as a function of irradiation time for the summer and autumn experiments, respectively. Because not all standards were available, other congeners were identified only within structural isomer groups (e.g., octabromodiphenyl ether, abbreviated as octaBDE) if they possessed very similar GC/MS retention times to those of the standards and if their mass spectra contained distinctive

TABLE 1. Relative Retention Times and Response Factors[a]

BDE number	IUPAC name	RT GC-ECD (min)	RT GC-ECD range (min)	RT GC−MS (min)	RT GC−MS range (min)	av RF GC-ECD	Br atoms
BDE1	2-bromodiphenyl ether	0.89	0.89−0.96	0.90	0.90−0.96	0.095	1
BDE2	3-bromodiphenyl ether	0.93		0.93			
BDE3	4-bromodiphenyl ether	0.96		0.96			
BDE7	2,4-dibromodiphenyl ether	1.64	1.46−1.84	1.33	1.24−1.44	0.29	2
BDE8	2,4′-dibromodiphenyl ether	1.71		1.38			
BDE10	2,6-dibromodiphenyl ether	1.46		1.24			
BDE11	3,3′-dibromodiphenyl ether	1.71		1.38			
BDE12	3,4-dibromodiphenyl ether	1.77		1.40			
BDE13	3,4′-dibromodiphenyl ether	1.77		1.41			
BDE15	4,4′-dibromodiphenyl ether	1.84		1.44			
BDE17	2,2′,4-tribromodiphenyl ether	2.48	2.18−2.72	1.73	1.75−1.86	0.49	3
BDE25	2,3′,4-tribromodiphenyl ether	2.48		1.74			
BDE28	2,4,4′-tribromodiphenyl ether	2.58		1.78			
BDE30	2,4,6-tribromodiphenyl ether	2.18		1.59			
BDE32	2,4′,6-tribromodiphenyl ether	2.40		1.70			
BDE33	2,3′,4′-tribromodiphenyl ether	2.58		1.78			
BDE35	3,3′,4-tribromodiphenyl ether	2.64		1.82			
BDE37	3,4,4′-tribromodiphenyl ether	2.72		1.86			
BDE47	2,2′,4,4′-tetrabromodiphenyl ether	3.29	3.07−3.74	2.10	2.00−2.23	0.69	4
BDE49	2,2′,4,5′-tetrabromodiphenyl ether	3.18		2.05			
BDE66	2,3′,4,4′-tetrabromodiphenyl ether	3.39		2.15			
BDE71	2,3′,4′,6-tetrabromodiphenyl ether	3.20		2.06			
BDE75	2,4,4′,6-tetrabromodiphenyl ether	3.11		2.02			
BDE77	3,3′,4,4′-tetrabromodiphenyl ether	3.54		2.23			
BDE85	2,2′,3,4,4′-pentabromodiphenyl ether	4.21	3.81−4.25	2.54	2.24−2.47	0.89	5
BDE99	2,2′,4,4′,5-pentabromodiphenyl ether	3.95		2.40			
BDE100	2,2′,4,4′,6-pentabromodiphenyl ether	3.81		2.33			
BDE116	2,3,4,5,6-pentabromodiphenyl ether	4.00		2.43			
BDE118	2,3′,4,4′,5-pentabromodiphenyl ether	4.07		2.47			
BDE119	2,3′,4,4′,6-pentabromodiphenyl ether	3.85		2.35			
BDE126	3,3′,4,4′,5-pentabromodiphenyl ether	4.25		2.57			
BDE138	2,2′,3,4,4′,5′-hexabromodiphenyl ether	4.81	4.25−4.81	2.98	2.61−2.98	1.08	6
BDE153	2,2′,4,4′,5,5′-hexabromodiphenyl ether	4.56		2.76			
BDE154	2,2′,4,4′,5,6′-hexabromodiphenyl ether	4.36		2.61			
BDE155	2,2′,4,4′,6,6′-hexabromodiphenyl ether	4.25		2.54			
BDE156	2,3,3′,4,4′,5-hexabromodiphenyl ether	4.92		3.09			
BDE166	2,3,4,4′,5,6-hexabromodiphenyl ether	4.81		3.00			
BDE181	2,2′,3,4,4′,5,6-heptabromodiphenyl ether	5.43	4.97−5.69	3.71	3.11−3.80	1.28	7
BDE183	2,2′,3,4,4′,5′,6-heptabromodiphenyl ether	5.12		3.29			
BDE184	2,2′,3,4,4′,6,6′-heptabromodiphenyl ether	5.04		3.17			
BDE190	2,3,3′,4,4′,5,6-heptabromodiphenyl ether	5.47		3.81			
BDE191	2,3,3′,4,4′,5′,6-heptabromodiphenyl ether	5.28		3.50			
BDE196	2,2′,3,3′,4,4′,5,6′-octabromodiphenyl ether	6.15	5.74−6.81	4.73	4.14−5.74	1.48	8
BDE197	2,2′,3,3′,4,4′,6,6′-octabromodiphenyl ether	5.93		4.39			
BDE206	2,2′,3,3′,4,4′,5,5′,6-nonabromodiphenyl ether	8.02	7.39−8.02	7.53	6.55−7.53	1.68	9
BDE207	2,2′,3,3′,4,4′,5,6,6′-nonabromodiphenyl ether	7.58		6.81			
BDE208	2,2′,3,3′,4,5,5′,6,6′-nonabromodiphenyl ether	7.39		6.55			
BDE209	2,2′,3,3′,4,4′,5,5′,6,6′-decabromodiphenyl ether	10.89	10.89	11.81	11.81	1.88	10

[a] RF is relative response factor, normalized to response of BDE99. RT is relative retention time, normalized to retention time of hexachlorobenzene.

fragments, characteristic of these structural isomers. For example, for the octaBDEs, the GC/MS retention times ranged from 28.01 to 38.88 min, and characteristic fragments included those with m/z ratios of 801.4, 721.6, and 642. Therefore, any GC/MS peaks observed between 28.01 and 38.88 min and exhibiting mass spectra containing all three fragments listed previously, with no larger fragments present, were identified as octaBDE congeners. Because of potential coelution of structural isomers, the identification of all specific congeners listed in Tables 2 and 3, except for the nonaBDEs, are tentative pending confirmation of relative retention times of all 209 congeners. It is important to note however, that the protocol used herein for identifying these congeners is consistent with that used by most researchers who have identified some of these same congeners in environmental samples.

The formation and subsequent photodecomposition of these congeners is evident in Figures 3−5, where GC−MS chromatograms are shown that correspond to increasing time of solar irradiation. After 18 min of solar irradiation in early afternoon October sunlight, all three nonaBDEs and several octaBDEs appear. Less substituted congeners appear in succession as the irradiation time increases. There is a clear, inverse correlation between irradiation time and number of bromine atoms on the remaining congeners, and in general, the rate of photodecomposition of the remaining congeners decreases with decreasing bromine substitution. For example, hexaBDEs begin to appear after 153 min with several remaining after 34 h of irradiation. Photoreaction rates of many of the pentaBDEs and tetraBDEs are similarly slow.

The first step in the photochemical transformation of BDE209 is loss of one bromine atom, resulting in nonaBDEs (see Figure 3). As shown in Figure 3a, after 18 min of solar irradiation, a substantial quantity of all three nonaBDE congeners have formed, with peaks at 44.33 (BDE208), 46.09 (BDE207), and 50.98 min (BDE206). That the peaks at 50.98 and 46.09 min corresponded to BDE206, and BDE207 was confirmed by matching mass spectra to standards. The peak at 44.33 min was deduced to be BDE208 because of its proximity to the other two nonaBDEs and because it has

TABLE 2. BDE209 Solar Irradiation Products, July 2–23, 2003

irradiation time (min)	congeners with identical RTs as reaction products	Br atoms	cumulative no. of congeners
0	209	10	1
5	209	10	
	208, 207, 206	9	4
10	209	10	
	208, 207, 206	9	
	197, 196, four additional OCTAs	8	10
15	209	10	
	208, 207, 206	9	
	197, 196, four additional OCTAs	8	
	183, three additional HEPTAs	7	14
20	209	10	
	208, 207, 206	9	
	197, 196, four additional OCTAs	8	
	183, four additional HEPTAs	7	15
30	208, 207, 206	9	
	197, 196, four additional OCTAs	8	
	183, four additional HEPTAs	7	15
97	197, 196, three additional OCTAs	8	
	183, four additional HEPTAs	7	
	154, 153, 138, eight additional HEXAs	6	
	99	5	27
234	183, two additional HEPTAs	7	
	154, 153, 138, eight additional HEXAs	6	
	100, 99, 85, one additional PENTA	5	
	77, 71, 49, 47	4	34
365	183, one additional HEPTA	7	
	154, 153, 138, eight additional HEXAs	6	
	100, 99, 85, five additional PENTAs	5	
	77, 71, 49, 47, two additional TETRAs	4	
	37, 33 or 28, one additional TRI	3	43

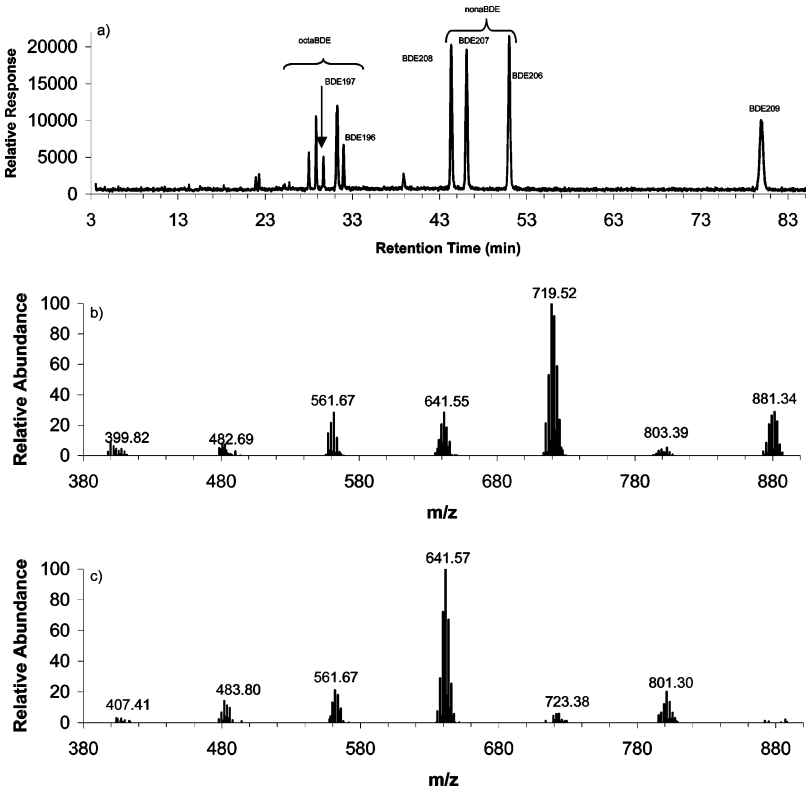

FIGURE 3. (a) GC–MS chromatogram after 18 min of BDE209 exposure to sunlight on October 23, 2003. (b) Mass spectrum of peak at 50.98 min, which matches that of BDE206. (c) Mass spectrum of peak at 32.00 min, which matches that of BDE196.

matching fragments at m/z ratios of 879.1, 721.5, and 641.6. Following the loss of the first bromine atom, continued debromination occurs at longer irradiation times, with congeners having three to nine bromine atoms observed. Figure 4 shows that significant formation of hexaBDEs and heptaBDEs occurs after 9 h of irradiation. Specifically, BDE183 and BDE153 were identified in samples irradiated for this length of time.

One of the most commonly detected PBDEs in the environment and in samples collected from organisms is

TABLE 3. BDE209 Solar Irradiation Products, October 23 to November 3, 2003

irradiation time (min)	congeners detected or identified	Br atoms	cumulative no. of congeners
0	209	10	1
18	209	10	
	208, 207, 206	9	
	197, 196, four additional OCTAs	8	
	183, one additional HEPTA	7	12
26	209	10	
	208, 207, 206	9	
	197, 196, four additional OCTAs	8	
	183, three additional HEPTAs	7	14
36	208, 207, 206	9	
	197, 196, four additional OCTAs	8	
	183, three additional HEPTAs	7	14
45	208, 207, 206	9	
	197, 196, four additional OCTAs	8	
	183, four additional HEPTAs	7	15
60	208, 207, 206	9	
	197, 196, four additional OCTAs	8	
	183, four additional HEPTAs additional	7	15
153	206	9	
	197, 196, three additional OCTAs	8	
	183, five additional HEPTAs	7	
	153, one additional HEXA	6	18
532	183, three additional HEPTA	7	
	154, 153, 138, eight additional HEXAs	6	
	118, 100, 99, two additional PENTAs	5	
	66, 49, 47	4	35
1200	183, one additional HEPTA	7	
	154, eight additional HEXA	6	
	118, 100, 99 one additional PENTA	5	
	66, 49, 47, one additional TETRA	4	36
2028	one HEPTA	7	
	154, seven additional HEXAs	6	
	118, 100, 99, two additional PENTAs	5	
	77, 66, 49, 47, two additional TETRAs	4	
	37, 33/28, one additional TRI	3	41

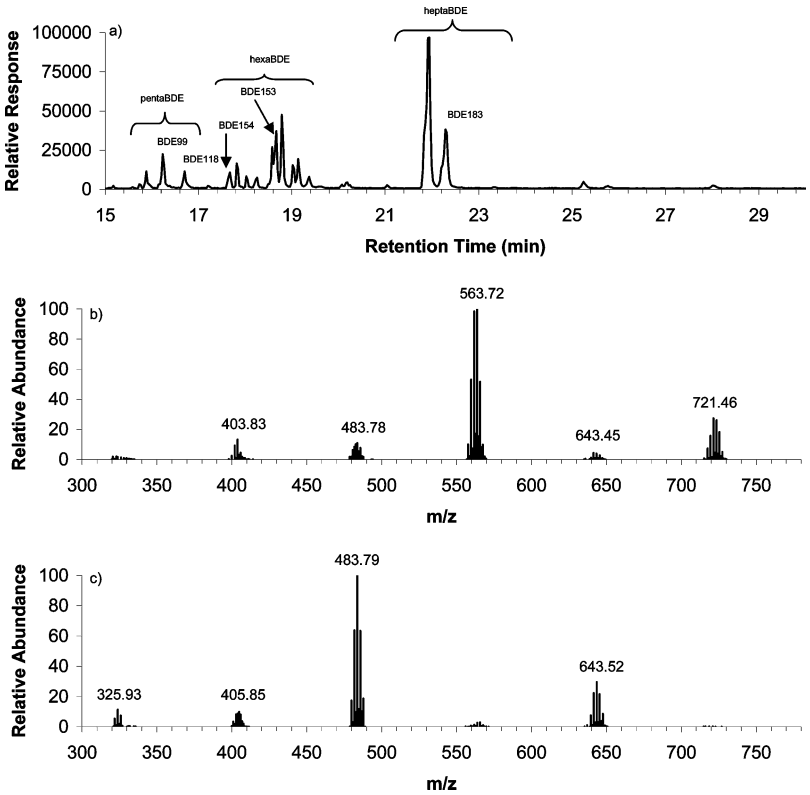

FIGURE 4. (a) GC–MS chromatogram after 9 h of BDE209 exposure to sunlight on October 23, 2003. (b) Mass spectrum of peak at 22.26 min, which matches that of BDE183. (c) Mass spectrum of peak at 18.65 min, which matches that of BDE153.

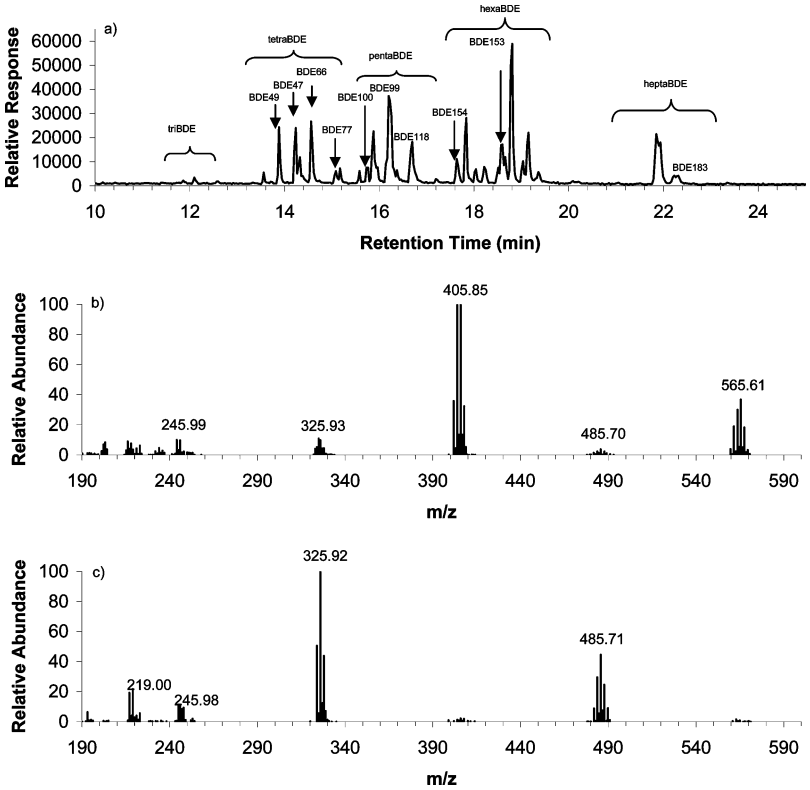

FIGURE 5. (a) GC−MS chromatogram after 27.8 h of BDE209 exposure to sunlight on October 23−29, 2003. (b) Mass spectrum of peak at 16.23 min, which matches that of BDE99. (c) Mass spectrum of peak at 14.22 min, which matches that of BDE47.

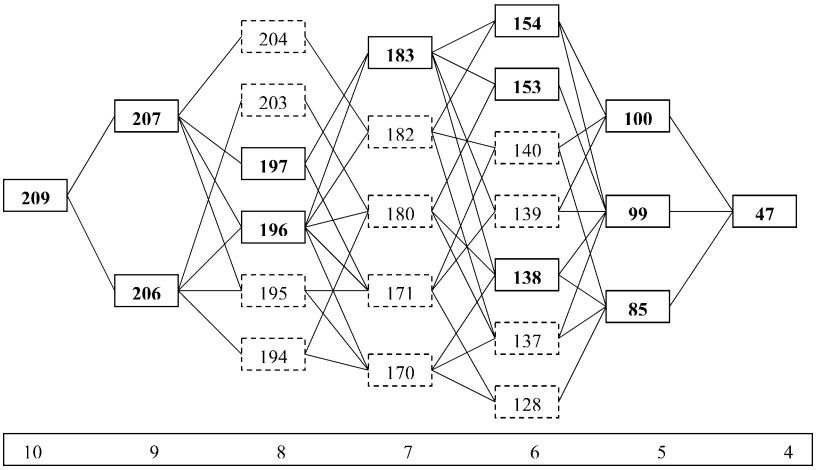

FIGURE 6. All potential intermediates in reductive debromination of DBE209 leading to BDE47. Congeners identified in solar irradiated samples in this study are indicated in the solid boxes.

2,2′,4,4′-tetrabromodiphenyl ether (BDE47). Thus, it is particularly interesting that irradiation of BDE209 leads to BDE47, detected after 20 h of solar irradiation in July (Table 2) and after 27.8 h of irradiation in October (Figure 5). It should be noted that of the 209 congeners within this class, 42 are tetra-isomers, with seven of these observed as products/intermediates in our experiments. The mass spectra of this product peak is identical to that of the BDE47 standard; however, it remains possible that coelution of another tetra congener may occur at this retention time, although there is no evidence of this from the shape of the peak or from the fragmentation pattern. Additional evidence to support the identification of this peak as BDE47 is the presence of all three potential pentaBDE precursor compounds on the chromatograms: BDE100, BDE99, and BDE85 (Table 2) and the potential presence of a debromination product, BDE28. The identity of the latter is equivocal due to the coelution of BDE33. Figure 6 shows all the potential intermediates in the reductive debromination of BDE209 leading to BDE47 and indicates those intermediates identified in this study.

To further examine overall product distribution, all peak areas within the RT ranges of each structural isomer group (Table 1) were quantified with the average RF of the known (standard) isomers. The total estimated concentration of reaction intermediates for each structural isomer group for the October experiment is shown in Figure 7. Because response factors vary among isomers, the resulting overall mass balance over time varies by as much as 30%. However, Figure 7 clearly shows the initial fast disappearance of BDE209 is matched by the initially rapid formation of nonaBDEs. The other congeners (octaBDEs, heptaBDEs, and hexaBDEs) accumulate successively over the 60 min exposure period, as octaBDEs are transformed to heptaBDEs that are then transformed to hexaBDEs.

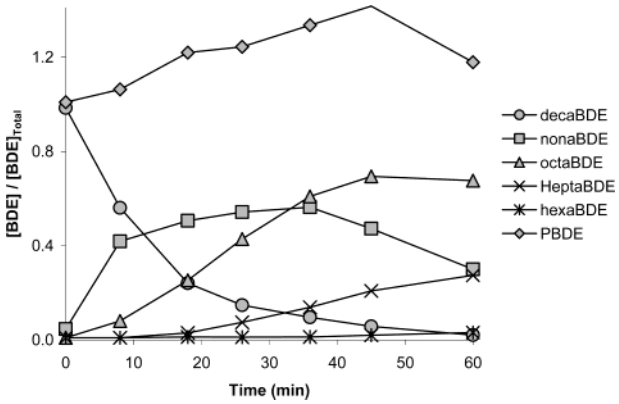

FIGURE 7. BDE209 product distribution, irradiated in hexane on October 23, 2003.

In additional experiments, BDE-156, -184, -191, -196, -197, -206, and -207 dissolved in hexanes were exposed individually to solar radiation (0−4 h) for reactivity and product analysis. Comparable appearance of less substituted PBDEs was observed in all cases, with greatest reactivity apparent for those congeners fully substituted in all ortho positions. Whether this is a result of higher quantum yields or molar absorptivities of these congeners is unknown.

In conclusion, rapid solar photoreduction of BDE209 in hexane with concomitant formation and subsequent decay of debromination products is shown to occur. The reaction rate in natural waters can be expected to be attenuated by sorption of BDE209 onto colloidal particles, by light attenuation by humic materials, and by the occurrence of lower concentrations and/or less favorable hydrogen donors (i.e., humic acids and water vs hexane). In a previous paper (*35*), we have shown that photodegradation occurs when hydrated precipitates of BDE209 are irradiated with solar light. Under these conditions, the reaction is much slower—on the order of days rather than minutes—resulting in Br^- accumulation in the aqueous phase and likely the polymerization of diphenyl ether moieties in the solid phase. Upon addition of humic substances to the aqueous phase, increased accumulation of nonaBDEs and octaBDEs occurred (*35*). In ongoing studies, we are examining the photoreactivity of BDE209 dissolved in humic acid solutions. Early results indicate that similar initial products are formed (e.g., all three nonaBDEs, BDE183, BDE153), again over periods of days rather than minutes. Clearly, there is a fairly significant solvent effect on reaction rate; however, solvent effects on overall reaction pathways and product distributions require additional attention.

Acknowledgments

This work was supported by the U.S. Environmental Protection Agency STAR Grants Program (Award R-83039801-0). The authors thank Dr. Changhe Xiao for technical assistance. This work was also supported in part by Purdue University, through a Ross Graduate Fellowship awarded to J.B.-C.

Literature Cited

(1) Matscheko, N.; Tysklind, M.; De Wit, C.; Bergek, S.; Andersson, R.; Sellstrom, U. *Environ. Toxicol. Chem.* **2002**, *21*, 2515−2525.
(2) Lacorte, S.; Guillamon, M.; Martinez, E.; Viana, P.; Barcelo, D. *Environ. Sci. Technol.* **2003**, *37*, 892−898.
(3) Rayne, S.; Ikonomou, M. G.; Antcliffe, B. *Environ. Sci. Technol.* **2003**, *37*, 2847−2854.
(4) Zegers, B. N.; Lewis, W. E.; Booij, K.; Smittenberg, R. H.; Boer, W.; De Boer, J.; Boon, J. P. *Environ. Sci. Technol.* **2003**, *37*, 3803−3807.
(5) Petrovic, M.; Eljarrat, E.; Lopez de Alda, M. J.; Barcelo, D. *Trends Anal. Chem.* **2001**, *20*, 637−648.
(6) Sellstrom, U.; Kierkegaard, A.; De Witt, C.; Jansson, B. *Environ. Toxicol. Chem.* **1998**, *17*, 1065−1072.
(7) Gouin, T.; Thomas, G. O.; Cousins, I.; Barber, J.; Mackay, D.; Jones, K. C. *Environ. Sci. Technol.* **2002**, *36*, 1426−1434.
(8) Strandberg, B.; Dodder, N. G.; Basu, I.; Hites, R. A. *Environ. Sci. Technol.* **2001**, *35*, 1078−1083.
(9) Jaward, F. M.; Farrar, N. J.; Harner, T.; Sweetman, A. J.; Jones, K. C. *Environ. Sci. Technol.* **2004**, *38*, 34−41.
(10) Lindberg, P.; Sellstrom, U.; Haggberg, L.; De Wit, C. A. *Environ. Sci. Technol.* **2004**, *38*, 93−96.
(11) Zennegg, M.; Kohler, M.; Gerecke, A. C.; Schmid, P. *Chemosphere* **2003**, *51*, 545−553.
(12) Voorspoels, S.; Covaci, A.; Schepens, P. *Environ. Sci. Technol.* **2003**, *37*, 4348−4357.
(13) Sellstrom, U.; Bignert, A.; Kierkegaard, A.; Haggberg, L.; De Wit, C. A.; Olsson, M.; Jansson, B. *Environ. Sci. Technol.* **2003**, *37*, 5496−5501.
(14) She, J.; Petreas, M.; Winkler, J.; Visita, P.; McKinney, M.; Kopec, D. *Chemosphere* **2002**, *46*, 697−707.
(15) Rice, C. P.; Chernyak, S. M.; Begnoche, L.; Quintal, R.; Hickey, J. *Chemosphere* **2002**, *49*, 731−737.
(16) Luross, J. M.; Alaee, M.; Sergeant, D. B.; Cannon, C. M.; Whittle, D. M.; Solomon, K. R.; Muir, D. C. G. *Chemosphere* **2002**, *46*, 665−672.
(17) Law, R. J.; Allchin, C. R.; Bennett, M. E.; Morris, S.; Rogan, E. *Chemosphere* **2002**, *46*, 673−681.
(18) Boon, J. P.; Lewis, W. E.; Tjoen-A-Choy, M. R.; Allchin, C. R.; Law, R. J.; De Boer, J.; Ten Hallers-Tjabbes, C. C.; Zegers, B. N. *Environ. Sci. Technol.* **2002**, *36*, 4025−4032.
(19) Hites, R. A. *Environ. Sci. Technol.* **2004**, *38*, 945−956.
(20) Ikonomou, M. G.; Rayne, S.; Addison, R. F. *Environ. Sci. Technol.* **2002**, *36*, 1886−1892.
(21) Barring, H.; Bucheli, T.; Broman, D.; Gustafsson, O. *Chemosphere* **2002**, *49*, 515−523.
(22) Harner, T.; Shoeib, M. *J. Chem. Eng. Data* **2002**, *47*, 228−232.
(23) Wong, A.; Lei, Y. D.; Alaee, M.; Wania, F. *J. Chem. Eng. Data* **2001**, *46*, 239−242.
(24) Butt, C. M.; Diamond, M. L.; Truong, J.; Ikonomou, M. G.; Schere, A. F. H. T. *Environ. Sci. Technol.* **2004**, *38*, 724−731.
(25) Chen, J. W.; Harner, T.; Yang, P.; Quan, X.; Chen, S.; Schramm, K.-W.; Kettrup, A. *Chemosphere* **2003**, *51*, 577−584.
(26) Wania, F.; Lei, Y. D.; Harner, T. *Anal. Chem.* **2002**, *74*, 3476−3483.
(27) Tittlemier, S. A.; Halldorson, T.; Stern, G. A.; Tomy, G. T. *Environ. Toxicol. Chem.* **2002**, *21*, 1804−1810.
(28) Hale, R. C.; Laguardia, M. J.; Harvey, E. P.; Gaylor, M. O.; Mainor, T. M.; Duff, W. H. *Nature* **2001**, *412*, 140−141.
(29) Sjodin, A.; Jakobsson, E.; Kierkegaard, A.; Marsh, G.; Sellstrom, U. *J. Chomatogr.* **1998**, *A822*, 83−89.
(30) Alaee, M.; Arias, P.; Sjodin, A.; Bergman, A. *Environ. Int.* **2003**, *29*, 683−689.
(31) BSEF, 2003. Major Brominated Flame Retardants Volume Estimates, January 21, 2003; www.bsef.com/newsite/bsef_frameset.html, accessed April 1, 2003.
(32) Stapleton, H. M.; Alaee, M.; Letcher, R. J.; Baker, J. E. *Environ. Sci. Technol.* **2004**, *38*, 112−119.
(33) Marsh, G.; Athanasiadou, M.; Bergman, A.; Asplund, L. *Environ. Sci. Technol.* **2004**, *38*, 10−18.
(34) Soderstrom, G.; Sellstrom, U.; Wit, C. A. D.; Tysklind, M. *Environ. Sci. Technol.* **2004**, *38*, 127−132.
(35) Hua, I.; Kang, N.; Jafvert, C. T.; Fabrega-Duque, J. R. *Environ. Toxicol. Chem.* **2003**, *22*, 798−804.
(36) Watanabe, I.; Tatsukawa, R. *Bull. Environ. Contamin. Toxicol.* **1987**, *39*, 953−959.
(37) Leifer, A. *The Kinetics of Environmental Aquatic Photochemistry: Theory and Practice*; American Chemical Society: Washington DC, 1988.

Received for review March 12, 2004. Revised manuscript received May 14, 2004. Accepted May 17, 2004.

ES049608O